

Space grid analysis method in modelling shear lag of cable-stayed bridge with corrugated steel webs

Ye Ma^{1a}, Ying-Sheng Ni^{*1}, Dong Xu^{2b} and Jin-Kai Li^{3c}

¹ Research Institute of Highway Ministry of Transport, M.O.T., Beijing, 100088, P.R. China

² Department of Bridge Engineering, Tongji University, Shanghai, 200092, P.R. China

³ China Railway Engineering Design Consulting Group Co., Ltd, Beijing, 100055, P.R. China

(Received December 27, 2016, Revised March 13, 2017, Accepted May 09, 2017)

Abstract. As few multi-tower single-box multi-cell cable-stayed bridges with corrugated steel webs have been built, analysis is mostly achieved by combining single-girder model, beam grillage model and solid model in support of the design. However, such analysis methods usually suffer from major limitations in terms of the engineering applications: single-girder model fails to account for spatial effect such as shear lag effect of the box girder and the relevant effective girder width and eccentric load coefficient; owing to the approximation in the principle equivalence, the plane grillage model cannot accurately capture shear stress distribution and local stress state in both top and bottom flange of composite box girder; and solid model is difficult to be practically combined with the overall calculation. The usual effective width method fails to provide a uniform and accurate “effective length” (and the codes fail to provide a unified design approach at those circumstance) considering different shear lag effects resulting from dead load, prestress and cable tension in the construction. Therefore, a novel spatial grid model has been developed to account for shear lag effect. The theoretical principle of the proposed spatial grid model has been elaborated along with the relevant illustrations of modeling parameters of composite box girder with corrugated steel webs. Then typical transverse and longitudinal shear lag coefficient distribution pattern at the side-span and mid-span key cross sections have been analyzed and summarized to provide reference for similar bridges. The effectiveness and accuracy of spatial grid analysis methods has been finally validated through a practical cable-stayed bridge.

Keywords: shear lag coefficient; cable-stayed bridge; spatial grid model; corrugated steel web; composite bridge girder

1. Introduction

Composite girder bridge with corrugated steel webs is a new type of composite structure and has been widely used in recent years in Japan. The structure has been gradually used from simple-supported beam, continuous beam to extra-dosed cable-stayed bridge, cable-stayed bridge, etc. As the dead weight of composite box girder bridge with corrugated steel webs is about 20%~30% as much as that of the concrete one, it saves 20%~30% cost relative to steel box beam or concrete box beam with equivalent span (He *et al.* 2007). Similarly in China, more than 30 composite girder bridge with corrugated steel webs have been built or is under construction since 2005. The girder cross section of these bridges extends from the original single-box single-cell to single-box multi-cell and multi-box multi-cell. The width-span ratio of bridges is more than 0.5 in many cases. Long-span and super-wide bridges have also appeared, such as Himiyume Ohashi extra-dosed cable-stayed bridge in Japan (91.75 + 180 + 91.75) m (Maeda *et al.* 2005), Ritto

Bridge (137.6 + 170 + 115 + 67.6) m (Yasukawa 2003), Yahagigawa cable-stayed bridge (174.7 + 2 × 235 + 174.7) m (Otani and Arai 2006), six-tower cable-stayed bridge of Chaoyang Bridge in Nanchang (79 + 5 × 150 + 79) m (Wang *et al.* 2015), three-tower cable-stayed bridge of Henan (58 + 118 + 188 + 108) m (Liu *et al.* 2016).

Similar to common concrete box girder, the phenomenon of uneven distribution of bending stress, which is called as “shear lag effect”, exist on both top and bottom flanges of the box girder. Existing studies of shear lag effect mainly focus on single-box single-cell girder with vertical or inclined webs that are mostly used for the simple beam structure; however, studies on shear lag effect of single-box multi-cell cable-stayed bridge with corrugated steel webs (in super-wide form) is very rare (Kim *et al.* 2011, Li and Wang 2013, Oh *et al.* 2012). Therefore, it is necessary to analyze the shear lag effect of multi-box multi-cell cable-stayed bridge with corrugated steel webs.

Under the longitudinal bending, the normal stress resulted in the flange slab section is uniform along the flange width based on Euler beam theory in modeling of bending (i.e., shear effect is not modelled). However, in most practical cases especially for box beam with wide flange, shear deformation in the flange slab results in unevenly distributed normal stress along the width of flange slab, which is known as “shear lag effect”. If the normal stress at the intersection of flange slab and webs is greater

*Corresponding author, Ph.D., Professor,
E-mail: ys.ni@rioh.cn

^a Researcher, E-mail: y.ma@rioh.cn

^b Professor, E-mail: Xu_dong@tongji.edu.cn

^c Engineer, Master, E-mail: lijinkaicec@163.com

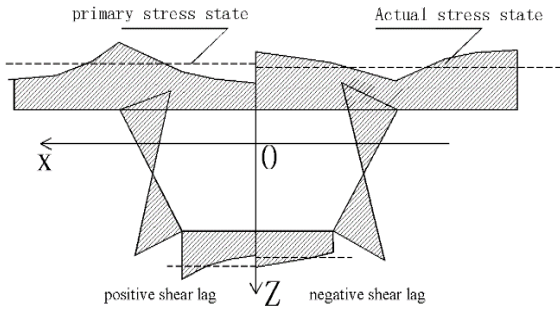


Fig. 1 Phenomenon of shear lag

than the stress calculated by Euler beam theory, it is called as “positive shear lag”; otherwise the “negative shear lag” (shown in Fig. 1). Such phenomenon of uneven distribution of normal stress can cause stress concentration and even cracking at the local intersection area between flanges and webs (Li and Wang 2013, Ko *et al.* 2013).

To account for the shear lag effect in design, the shear lag coefficient λ is defined as the ratio between the actual normal stress value and that calculated from the elementary beam theory. In this article, the normal stress calculated from the elementary beam theory is averagely calculated by area of normal stress of flange slab divided by width of flange slab. Then the shear lag coefficient at every point of cross sections can be obtained using its actual stress divided by the aforementioned average stress. Such shear lag coefficient is not only similar to the one by the classic definition but considers the features of spatial structure analysis, i.e.,

$$\sigma_0 = \sum_1^n \sigma_i b_i / b \tag{1}$$

Shear lag coefficient is calculated by $\lambda = \sigma/\sigma_0$ and the maximum shear lag coefficient is defined as $\lambda_{max} = \sigma_{max}/\sigma_0$, where σ_{max} is the average normal stress of three-dimensional solid unit node, b_i denotes the transverse distance of unit nodes, σ_{max} is the maximum stress of flange slab calculated by finite element method, σ_0 denotes the average normal stress calculated by the elementary beam theory, and n represents the number of units divided on top and bottom slab.

From Eq. (1) it can be seen that the effective flange width is determined based on the principle of equivalent volume of stress. The ratio of effective width to actual width (i.e., the effective width ratio) reflects the uneven distribution of normal stress across flange slab. At present in the bridge design, the reducing bending moment of cross section using the effective flange width based on which the bending stress and deflection of the beam are calculated through the elementary beam theory.

At present, for the analysis of composite girder bridge with corrugated steel web, the method combining the space frame model, plane beam grillage model and local solid model analysis is generally adopted. However, the spatial frame model lacks of the refinement analysis technique in considering the space effect, such as the plane section assumption of wide box girder, effective flange width, eccentric load coefficient, internal force distribution with

the webs, transverse vehicle distribution factor. Due to the approximation of equivalence principle, the plane beam grillage method cannot accurately reflect the shear stress distribution and local stress within the top and bottom plates of the composite box girder. The solid model is hard to be fully combined with the overall calculation as the resulting stress is not compatible with the responses required for design. Therefore the spatial grid model has been introduced to resolves these drawbacks for multi-box multi-cell composite girder with corrugated steel webs.

In the grid model, the composite beam section was separated into several plates, making the beam grillage division for each plate and equivalently replacing the stress of each plate by the divided beam grillage. Compared with the beam grillage method, the spatial grid division is much finer. Due to the denser division of the top plate, it can analyze the stress of the beam grillage of the top plate under the shear lag effect, without calculating the effective width. The output results of the spatial grid model are internal force, stress and displacement of each beam grillage. The torsion rigidity is reflected on the shear stress of each beam grillage through the mutual interaction between spatial grids. It can also achieve the distortion analysis of the cross section and the transverse flexural deformation of each plate, and can provide a comprehensive deformation analysis of the composite girder under eccentric load. The stress state of various structural components can be conveniently revealed for specific strengthening reinforcement, which is of prime significance in the practical engineering design (Shao *et al.* 2010).

2. The spatial grid model

In structural analysis, the complex bridge structure can be decomposed into several plates. Each plate element is composed of a crisscross orthogonal beam grillage with the cross beam rigidity (6 DOF beam element) equal the rigidity of the plate (seen in Fig. 2). The quantity of plates constituting a space bridge girder is equal to the number of crisscross beam grillage. Therefore, the spatial bridge structure can be modelled as a spatial grid structure. As shown in Fig. 2, the cross section of the single box girder

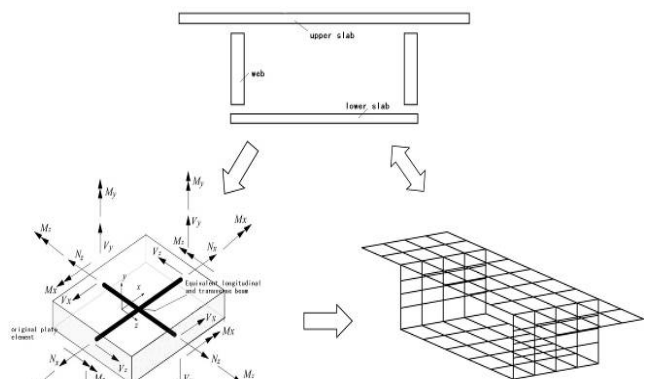


Fig. 2 Schematic show of spatial grid model

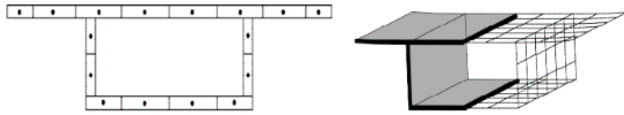


Fig. 3 Structure partitioning for box girder bridge in spatial grid model

can be decomposed into the top plate, bottom plate and webs. “Plate” of the box girder cross section can be modelled by the orthogonal beam grillage. The orthogonal beam grillages in different planes assemble the box girder as a spatial net structure, which is termed as “spatial grid” model (Liu and Xu 2010).

2.1 Structure partitioning

When building the spatial grid model, the longitudinal direction of the girder can be meshed in accordance with the usual meshing rules in finite element method for single-beam model. The refinement degree for grid across the cross section of girder should be determined in accordance with the cross section type and modelling requirements to reflect the space effect. The top and bottom flange plates and webs should be partitioned, as shown in Fig. 3.

2.2 Calculation of cross section characteristics after partitioning

In the spatial grid model for the box girders with webs, the cross section mainly includes the following three types shown in Fig. 4, i.e., the integral web part, partitioned parts of web, and partitioned parts of top and bottom plates. The calculation of these cross sections and characteristics is consistent with the cross section characteristics of the traditional beam element, which is calculated by the actual cross sectional dimension after dispersing.

A common rectangular partition shown in Fig. 5 is employed as an example to calculate the cross section

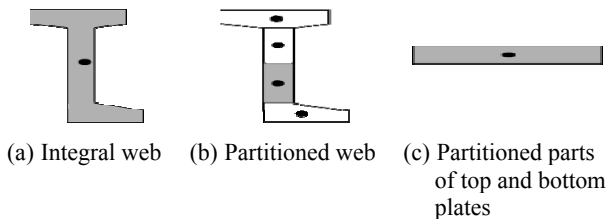


Fig. 4 Typical cross section in spatial grid model

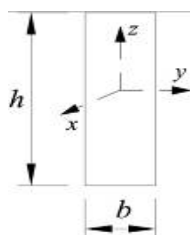


Fig. 5 Calculation of common cross section characteristics in spatial grid model

characteristics of typical parts in the spatial grid model.

Axial area

$$A_x = bh \tag{2}$$

Shear area

$$A_y = A_z = bh \tag{3}$$

Bending moment of inertia

$$I_z = \frac{b^3h}{12}; \quad I_y = \frac{bh^3}{12} \tag{4}$$

Torsional moment of inertia

$$I_T = \frac{4I_zI_y}{\beta(I_z + I_y)} \quad \beta = 1.3 \sim 1.6 \tag{5}$$

2.3 Calculation and modelling in spatial grid model

In the grid model, the composite beam section was separated into several plates, making the beam grillage division for each plate and equivalently replacing the stress of each plate by the divided beam grillage. Due to the denser division of the top plate, it can analyze the stress of the top plate under the shear lag effect, without calculating the effective width. The torsion rigidity is reflected on the shear stress of each beam grillage through the mutual interaction between spatial grids. It can also achieve the distortion analysis of the cross section and the transverse flexural deformation of each plate, and can provide a comprehensive deformation analysis of the composite girder under eccentric load.

While using the spatial grid model, the load effect of the cross section can be resisted respectively as: (1) The longitudinal effect of the box girder cross section (such as the axial force and bending moment) is resisted by longitudinal beam grillage; (2) The transverse effect of the box girder cross section (such as the distortion and transverse effect of live load) is achieved by transverse beam grillage; and (3) The torsion effects of the box girder cross section are transformed into shear force of the web beam grillage.

In the spatial grid model, the internal forces of the cross section are distributed to each partitioning parts in accordance with their rigidity. As shown in Fig. 6, the element is normally under axial forces N_x and N_y , in-plane shear forces V_{xy} and V_{yx} , and out-of-plane bending moment M_x and M_y . Under N_x and N_y , the in-plane membrane stress is distributed uniformly over the element thickness. The local load effect in top and bottom plates can be calculated bellows.

The out-of-plane normal stress under M_x and M_y can be obtained as

$$\sigma_x = \frac{M_y z}{I_y} \tag{6}$$

$$\sigma_y = \frac{M_x z}{I_x} \tag{7}$$

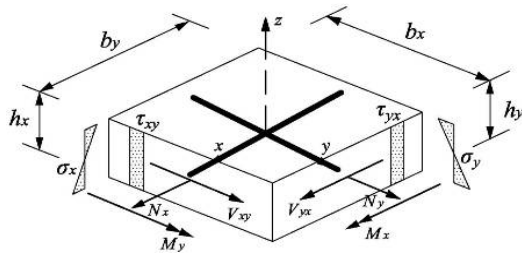


Fig. 6 Calculation of internal forces of elements in spatial grid model

where σ_x and σ_y are normal stress of the cross section under M_x and M_y , respectively; z is the perpendicular distance to the neutral axis; I_x and I_y are second moment of area about the neutral axis x and y , respectively; and M_x and M_y are the bending moment about the neutral axis x and y , respectively.

The in-plane normal stress can be calculated as

$$\sigma_{x-m} = \frac{N_x}{A_x} = \frac{N_x}{b_x h_x} \quad (8)$$

$$\sigma_{y-m} = \frac{N_y}{A_y} = \frac{N_y}{b_y h_y} \quad (9)$$

where σ_{x-m} and σ_{y-m} are the in-plane membrane stress in x and y direction, respectively; and b_x and b_y , h_x and h_y are elemental width and height in x and y directions, respectively.

The in-plane shear stress can be derived by

$$\tau_{xy} = \frac{V_{xy}}{b_x h_x} \quad (10)$$

and the in-plane principal tensile stress σ_t and compressive stress σ_c are derived by the following equation.

$$\sigma_t = \frac{\sigma_{x-m} + \sigma_{y-m}}{2} + \sqrt{\left(\frac{\sigma_{x-m} - \sigma_{y-m}}{2}\right)^2 + \tau_{xy}^2} \quad (11)$$

The output results of the spatial grid model are internal force, stress and displacement of each beam grillage. The stress state of various structural components can be conveniently and accurately revealed for specific strengthening reinforcement, which is of prime significance in the practical engineering design.

2.4 Application scope

The combined “plate” elements in spatial grid model provides unique bending, torsion and shear resistance resulting from the integral box cross section girder. These plates can be steel, concrete, or other composite materials such as steel concrete composite beam. The applicability of spatial grid model is not limited to specific structure form and it can be applied to various bridges including the curved, wide, and composite bridges.

2.5 Difference between the standard shear lag effect models and spatial grid model

Many researches have been conducted for shear lag effect of wide flange bridge and some of those results have been considered into the design codes using effective flange width. The effective flange is achieved through reduction of the section flange width in considering the unevenly distributed normal stress. However, this method can only consider the shear lag effect roughly and is only applicable to some simple structures under specific simplified loading.

For bridges with multi-web box beam, using of the effective width method fails to obtain a uniform and relatively accurate “effective width”. For example for cross section shown in Fig. 7, the shear lag effect due to dead load, prestress and cable tension are different in the construction process, and the code fails to provide a unified design approach at those circumstance. The shear lag effect due to the prestressed reinforcement and stayed cable is actually become the issue of how the point load transfers to the uniformly distributed across the section. It should be noted that shear lag effect is comparatively obvious for flat wide beam, and shear lag effect might be completely different even for identical cross section with different spans (Liu and Xu 2012).

The shear lag coefficient (or effective flange width) is highly dependent on the form of structure. At present, the methods recommended by codes are only applicable to specific structure state under vertical loading (i.e., under bending moment and moment from the prestressing), rather than for structure under longitudinal axial force (such as prestress induced axial force). If the shear lag coefficient for bridge under final operating state is adopted for the construction state, the consideration of shear lag effect will not be appropriate (Nie *et al.* 2011, Xu and Zhao 2012). For the bridge with composite girder, the single beam model based on elementary beam theory is mostly used. Based on the concept of effective flange width and equivalency between cross sections, the composite girder section is usually transformed into the I-shaped for analyze and design, as shown in Fig. 8. However, this approach has significantly ignored the spatial features of the internal forces and stress over the cross section. It not only fails to obtain a relatively accurate “effective width” but fails to consider the transverse shear stress in the concrete bridge deck, which significantly influences the reinforcement design for the composite girder slabs (Shan and Yan 2011,

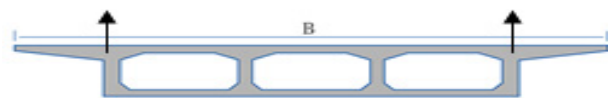


Fig. 7 Wide box girder cross section of a cable stayed bridge

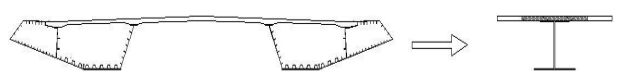


Fig. 8 Equivalent I cross section of the composite box girder

Jiang *et al.* 2013, Xu and Zhao 2012). In addition, the effective width method only focus on the normal stress of top and bottom plates and shear stress of web, rather than the shear stress and shear flow of top and bottom plates. This means that it fails to fully model the in-plane bi-axial stress state for top and bottom plates in reinforcement design. In practices, diagonal cracks owing to the bi-axial stress state are usually observed at the top and bottom plates but they are not considered in the traditional design and calculation based on elementary beam theory.

All the bridge deck structure can be divided into two kinds of basic stress element: In-plane stress elements of mid plane bear normal stress and in-plane shear stress, it is composed of the in-plane principal tensile stress and in-plane principal compressive stress (Xu and Zhao 2012), The sketch map of in-plane stress in the middle plane is shown in Fig. 9; Out-of-plane stress elements of upper and lower edge bear normal stress and out-of-plane shear stress, but the out-of-plane shear stress is smaller than the in-plane, The sketch map of out-of-plane stress in the upper and lower edge is shown in Fig. 10.

As seen in Fig. 11, in the spatial grid model a box girder section has been partitioned into N plate elements with complete in-plane and out-of-plane stress calculated. Each plate element comprises of three layers, the outer, middle and inner layers. Both of the inner and outer layers are one-dimensional normal stress region (with longitudinal and transverse stress) due to flexural moments while the middle layer is two-dimensional plane stress region with principal stress. A single cell box girder contains 9 complete checking

stress indices are shown in Table 1 along with the corresponding stress state, but in-plane stress of the top and bottom of box girder is not included in the current standard calculation system, also, caused lack of corresponding structure calculation and reinforcement method, The completed normal stress must be considered in the calculation of shear lag coefficient, which are often observed and common in engineering (Xu and Zhao 2012, Liu *et al.* 2015, He *et al.* 2012, Hassanein and Kharoob 2012).

The next section will use space mesh analysis method to make analysis of side-span and mid-span longitudinal and transverse distribution rules of shear lag coefficient for multi-box multi-cell wide box beam multi-tower cable-stayed bridge with corrugated steel webs.

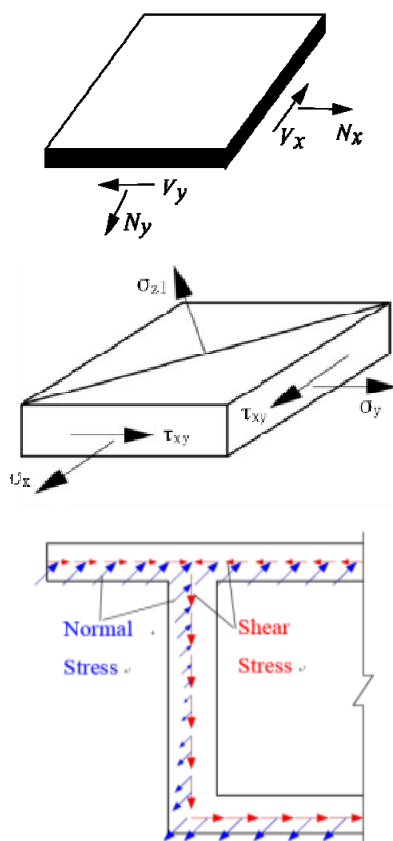


Fig. 9 The sketch map of in-plane stress in the middle plane

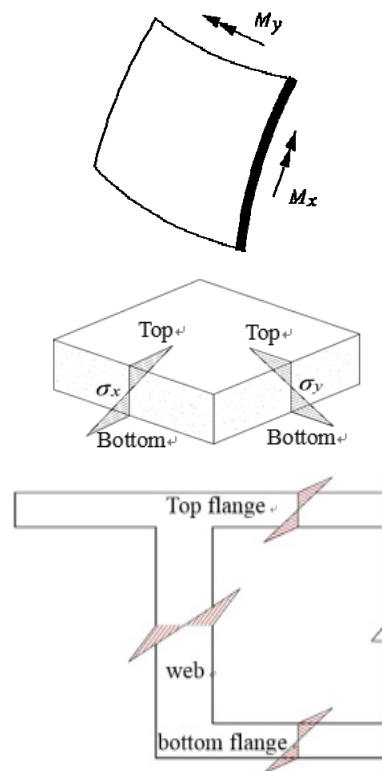


Fig. 10 The sketch map of out-of-plane stress in the upper and lower edge

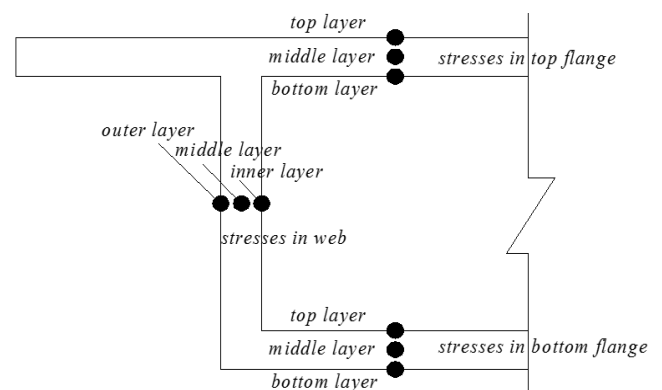


Fig. 11 Outer, middle, inner layers for top and bottom flange and webs

Table 1 A box girder contains 9 complete checking stress

Component/force direction	Position	Stress characteristics	Contrast with traditional stress
Out-of-plane of top flange	Top layer	Longitudinal normal stress	Upper surface stress of whole section
	Top layer	Transverse normal stress	In addition, local calculation of bridge deck is needed
	Bottom layer	Transverse normal stress	In addition, local calculation of bridge deck is needed
In-plane of top flange	Middle layer	Principal stress	Not contain (as the composite beam)
Out-of-plane of bottom flange	Bottom layer	Longitudinal normal stress	Lower surface stress of whole section
	Top layer	Transverse normal stress	The major is calculate the external collapse force of bottom slab
	Bottom layer	Transverse normal stress	Simplified calculation method is not perfect
In-plane of bottom flange	Middle layer	Principal stress	Not contain (as the composite beam)
In-plane of web	Middle layer	Principal stress	Web principal stress

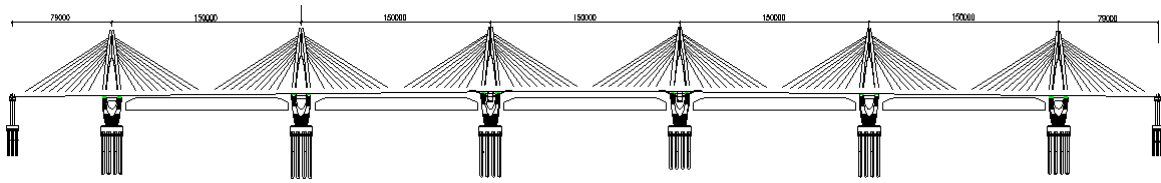


Fig. 12 Overall layout of the Chaoyang bridge

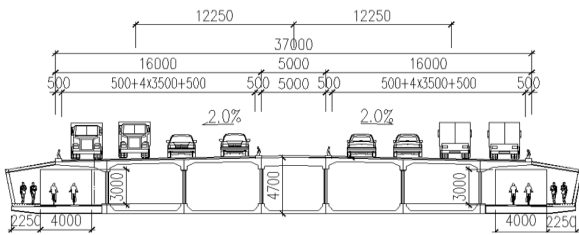


Fig. 13 Cross section of the bridge girder (in mm)



Fig. 14 Cross section of the corrugated steel webs (in mm)

lower and upper nodes of the web elements; for the single-beam part, the bridge support is connected to the nodes of girder through transverse rigid arm. The lower nodes of the link element in simulating bridge support are connected to the nodes of the cantilever element on top of the pier. The flexural stiffness of the support element is set to be zero. The global coordinate system of the bridge is defined as: the origin is set at the midpoint of end crossbeam on one side, x is along the longitudinal direction of the bridge, y is along the vertical direction which is opposite to the gravity direction, and z is along the transverse direction of the bridge. The bridge is modelled on finite element software platform WISEPLUS (www.wiseplus.cn).

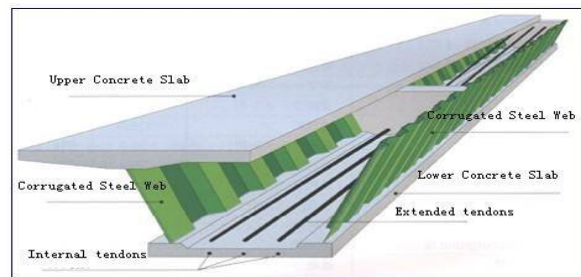
Fig. 17 presents the partition and nodes of box girder sections in which a total of 48 sub-plate elements are



(a) Overall layout



(b) Corrugated web



(c) Typical box girder with corrugated steel web

Fig. 15 The physical overall layout of Chaoyang Bridge

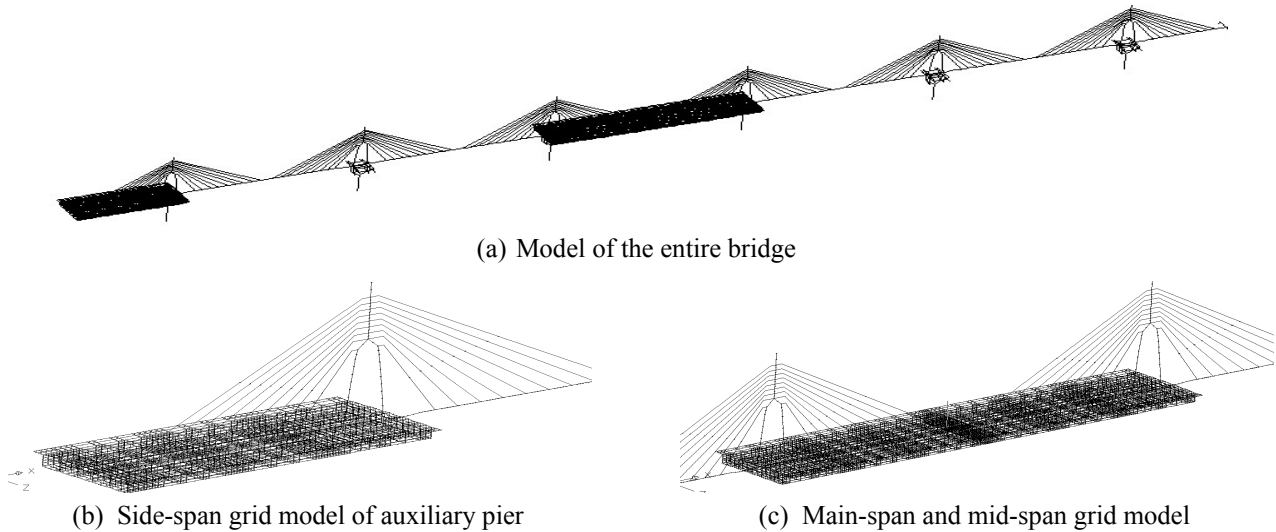


Fig. 16 The spatial grid model and single beam model

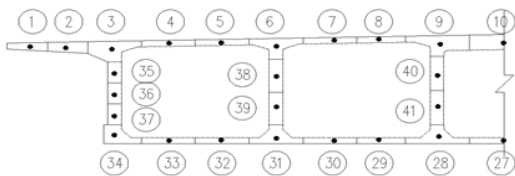


Fig. 17 Partition of the box girder section (symmetric)

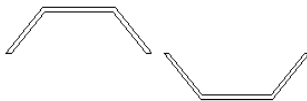


Fig. 18 Cross section of sub-web element

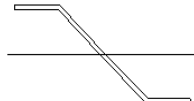


Fig. 19 Out-plane rigidity cross section of vertical bar

obtained. The corrugated webs are divided into 2 or 3 rectangular sub-web elements. The top and bottom slab are divided into multiple sub-slab elements. Both the in-plane and out-plane normal stresses as outlined in Table 1 can be obtained for these sub-elements at top and bottom flanges and steel webs. The numbers in the circles represent the identification number of the sub-elements while the solid dots denote the centroids of these sub-elements. In the spatial grid model, the cross section of vertical sub-web elements of the corrugated webs are shown in Fig. 18. The cross section corresponding to the web vertical bar unit chosen by out-plane rigidity is shown in Fig. 19.

The meshing scheme in the longitudinal direction (along the entire bridge) shown in Fig. 20 is used to model the transverse framing effect of the box girder at the location of the cross diaphragm girder. The similar meshing is used at the side 1st span and middle 4th span. The mesh refinement was conducted for the key segments 1#, 5# and 9# by considering the steel stiffening rib, steel cross-beam, virtual cross-beam, segment joint, etc. The stress and forces results in these key segments will be presented later in the context.

3.3 Shear lag coefficient distribution rules at side-span and mid-span

The shear lag effect of single-box multi-cell cross section of the cable-stayed bridge is accounted for by the shear lag coefficient. The loading on the bridge consider the self-weight, dead load and the simultaneous loading from longitudinal and transverse pre-stress and cable-stayed force on bridge deck after the entire construction support removal. By using the proposed theoretical spatial grid model in Section 2, the shear lag coefficient at key locations are calculated and its distribution rules are investigated for two operating conditions of the bridges. Table 2 presents the shear lag coefficient across the box-girder cross section for every sub-element on the flanges and webs under self-weight, dead load, pre-stress and cable force.

For the key segment (mesh refinement area) 1 at side-span under self-weight effect, it is seen that sub-elements 3 and 6 at top slab and 28 at bottom slab have positive shear lag, while sub-element 9 of top flange and 34 and 31 of the

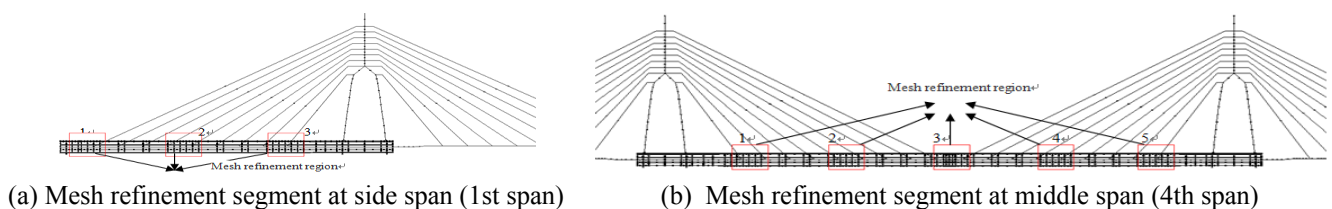


Fig. 20 Schematic diagram of mesh encryption area in the middle and side span

Table 2 Shear lag coefficient distribution over cross section at key longitudinal locations of bridge

Load case and location	Key segment 1	Key segment 3
Self-weight Side-span		
Self-weight Mid-span		
Dead load + prestress + cable force Side-span		
Dead load + prestress + cable force Mid-span		

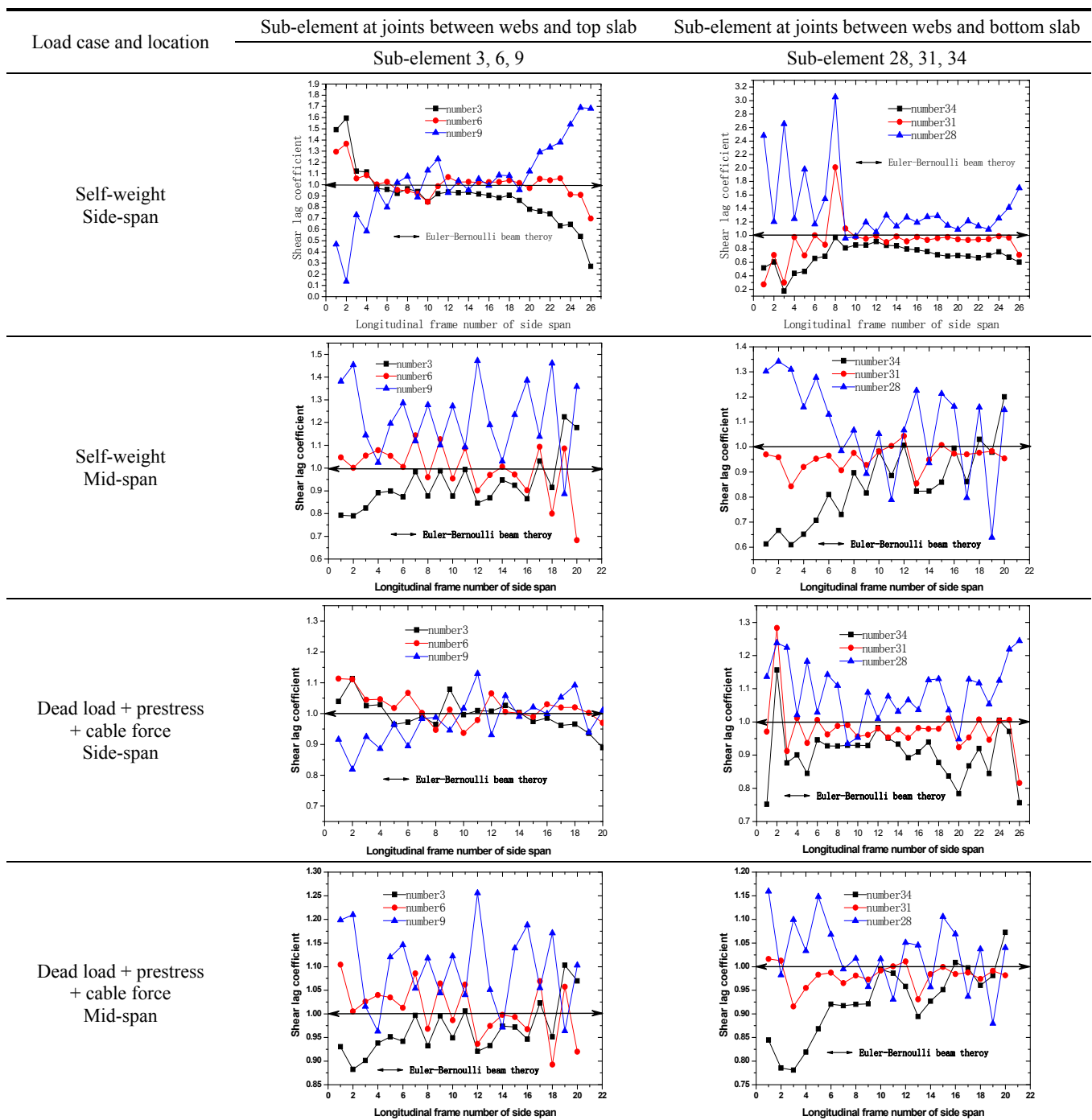
bottom slab have negative shear lag. In the key segment 3 of side span under self-weight, sub-element 3 of top slab and 34 and 31 of bottom slab have negative shear lag, while sub-element 6 and 9 of top slab and 28 of bottom slab have positive shear lag. For the key segment (mesh refinement area) 1 at mid-span under self-weight, sub-element 3 in top slab and 34 and 31 of bottom slab have negative shear lag coefficient while sub-element 6 and 9 of top slab and 28 of bottom slab have positive shear lag coefficient. Alternation between positive and negative shear lag effect occurs at both the top and bottom slab at side-span and mid-span cross sections among webs. The shear lag effect rules differ from that of a general common box girder with positive shear lag at the joint between webs and top slab and negative shear lag at the flange areas away from the webs. This is because the loading effect resulting from the existing stayed cables. In addition, under the self-weight loading, the shear lag coefficient at side-span and mid-span cross sections of cable-stayed bridge with corrugated steel

webs shows irregular distribution pattern.

Under the dead-weight and pre-stress load, it is seen that the distribution rule of shear lag coefficient on cross sections of side-span and mid-span mesh refined regions is almost consistent with that of under the dead-weight, indicating that pre-stress load plays minor effect on the distribution rule of shear lag coefficient. Owing to the role of stayed cable, the shear lag coefficient of cross sections of composite girder bridge with corrugated steel webs shows irregular distribution pattern.

For the key segment (mesh refinement area) 1 at side-span under self-weight effect, it is seen that sub-elements 3 and 6 at top slab and 28 at bottom slab have positive shear lag, while sub-element 9 of top flange and 34 and 31 of the bottom slab have negative shear lag. In the key segment 3 of side span under self-weight, sub-element 3 of top slab and 34 and 31 of bottom slab have negative shear lag, while sub-element 6 and 9 of top slab and 28 of bottom slab have positive shear lag. For the key segment (mesh refinement

Table 3 Shear lag coefficient distribution in the longitudinal direction



area) 1 at mid-span under self-weight, sub-element 3 in top slab and 34 and 31 of bottom slab have negative shear lag coefficient while sub-element 6 and 9 of top slab and 28 of bottom slab have positive shear lag coefficient. Alternation between positive and negative shear lag effect occurs at both the top and bottom slab at side-span and mid-span cross sections among webs. The shear lag effect rules differ from that of a general common box girder with positive shear lag at the joint between webs and top slab and negative shear lag at the flange areas away from the webs. This is because the loading effect resulting from the existing stayed cables. In addition, under the self-weight

loading, the shear lag coefficient at side-span and mid-span cross sections of cable-stayed bridge with corrugated steel webs shows irregular distribution pattern.

Under the dead-weight and pre-stress load, it is seen that the distribution rule of shear lag coefficient on cross sections of side-span and mid-span mesh refined regions is almost consistent with that of under the dead-weight, indicating that pre-stress load plays minor effect on the distribution rule of shear lag coefficient. Owing to the role of stayed cable, the shear lag coefficient of cross sections of composite girder bridge with corrugated steel webs shows irregular distribution pattern.

4. Conclusions

To resolve the drawbacks of common bridge design approach including the single-girder model, plane beam grillage model and solid model, a novel spatial grid model has been developed to account for shear lag effect of the cable stayed bridge with box girder and corrugated steel webs. A practical cable-stayed bridge with six tower has been adopted as numerical examples to validate the practical application of the proposed model. Then typical transverse and longitudinal shear lag coefficient distribution pattern at the side-span and mid-span key cross sections have been analyzed and summarized to provide reference for similar bridges. The following conclusions have been drawn from this research:

- As few cable-stayed bridges with corrugated steel webs have been built and multi-tower cable-stayed bridges are even fewer, single-girder and solid model are combined design calculation. It cannot achieve the purpose of refinement design to use shear lag coefficient to consider effective distribution width of sections by mainly imitating empirical value for concrete box beam, empirical value or trial value for similar engineering. But spatial grid analysis method can get the results required for every sub-element in top and bottom slabs to achieve refined calculation and design. For the shear lag coefficient analyzed for the single-box multi-cell girder with corrugated steel webs for a six-tower cable stayed bridge, we can take 2.37 for the maximum positive shear lag coefficient of side span and 0.437 for the minimum negative shear lag coefficient; and we can take 1.47 for the maximum positive shear lag coefficient of mid span and 0.75 for the minimum negative shear lag coefficient.
- In the spatial grid model, the top and bottom flanges and webs of the box girder have been partitioned into many sub-elements, thereby a complete stress results can be derived and these stress indices are consistent with practical engineering crack pattern and these outputs are of prime significance in practical bridge design. Such common methods in accounting for the shear lag effect, like the effective distribution method, cannot achieve it.
- Through demonstration by a practical bridge calculation, spatial grid model can provide the complete stress of single-box multi-cell box girder of a cable stayed bridge under the dead load and pre-stress effects. Shear lag effect of top and bottom slab in the side-span and mid-span key cross sections has been investigated. Through the analysis, it concludes the distribution rule of shear lag effect in key cross sections, the longitudinal distribution rule of shear lag coefficient, etc., verifies effectiveness and accuracy of spatial grid method and provides meaningful guidance for refinement design.
- The spatial grid model can resolves the deficiencies of single-girder model, plane beam grillage model and solid model. From the point of completeness of analysis and stress checking, it develops new thought

for refinement design..

Acknowledgments

This study was conducted at Research Institute of Highway Ministry of Transport, China and was supported by National Natural Science Foundation of China under Grant No. 51178335. The authors thank the anonymous reviewers and the Editor for their constructive comments and advice, which greatly improved the quality of this manuscript.

References

- Hassanein, M.F. and Kharoob, O.F. (2013), "Behavior of bridge girders with corrugated webs: (II) Shear strength and design", *Eng. Struct.*, **57**, 544-543.
- He, J., Chen, A. and Liu, Y. (2007), "Analysis on structural system and mechanical behavior of box girder bridge with corrugated steel webs", *Proceedings of the 3rd International Conference on Steel and Composite Structures (ICSC07)*, Manchester, UK, July-August, pp. 489-494.
- He, J., Liu, Y., Chen, A. and Yoda, T. (2012), "Mechanical behavior and analysis of composite bridges with corrugated steel webs: State-of-the-art", *Int. J. Steel Struct.*, **12**(3), 321-338.
- Jiang, L., Qi, J., Scanlon, A. and Sun, L. (2013), "Distortional and local buckling of steel-concrete composite box-beam", *Steel Compos. Struct., Int. J.*, **14**(3), 243-265.
- Kim, K.S., Lee, D.H., Choi, S.M., Choi, Y.H. and Jung, S.H. (2011), "Flexural behavior of prestressed composite beams with corrugated web: part I. Development and analysis", *Composites: Part B*, **42**(6), pp. 1603-1616.
- Ko, H.J., Moon, J., Shin, Y.W. and Lee, H.E. (2013), "Non-linear analyses model for composite box-girders with corrugated steel webs under torsion", *Steel Comp. Struct., Int. J.*, **14**(5), 409-429.
- Li, G.Q. and Wang, W.Y. (2013), "A simplified approach for fire-resistance design of steel-concrete composite beams", *Steel Comp. Struct., Int. J.*, **14**(3), 295-312.
- Liu, C. and Xu, D. (2010), "Space frame lattice model for stress analysis of bridge", *Baltic J. Road Bridge Eng.*, **5**(2), pp. 98-103.
- Liu, C. and Xu, D. (2012), "Influence of cracking on deflections of concrete box girder bridges", *Baltic J. Road Bridge Eng.*, **7**(2), 104-111.
- Liu, X.G., Fan, J.S., Nie, J.G., Bai, Y., Han, Y.X. and Wu, W.H. (2015), "Experimental and analytical studies of prestressed concrete girders with corrugated steel webs", *Mater. Struct.*, **48**(8), 2505-2520.
- Liu, W., Zhang, F., Li, P., Zhang, R. and Wan, S. (2016), "Mechanical analysis of prestressed concrete partially cable-stayed bridge with corrugated steel webs", *Advances in Engineering Research, Proceedings of the 4th International Conference on Sustainable Energy and Environmental Engineering (ICSEEE 2015)*, Shenzhen, China, December, pp. 166-170.
- Maeda, Y., Iijima, M. and Asai, H. (2005), "The extradosed cable anchorage and ultimate behavior for extradosed bridge with corrugated steel webs", *Proceeding of JSCE*, **794**, 227-238.
- Nie, J., Tao, M., Cai, C.S. and Li, S. (2011), "Analytical and numerical modeling of prestressed continuous steel-concrete composite beams", *J. Struct. Eng. ASCE*, **137**(12), 1405-1428.
- Oh, J.Y., Lee, D.H. and Kim, K.S. (2012), "Accordion effect of

- prestressed steel beams with corrugated webs”, *Thin-Wall. Struct.*, **57**, 49-61.
- Otani, M. and Arai, T. (2006), “Outline of TOYOTA-Arrows-Bridge”, Technical Report of Kawada Construction Co. LTD.; Volume 25, pp. 48-53.
- Shan, C.L. and Yan, L. (2011), “Creep stress analysis of PC composite box girder bridge with corrugated steel webs”, *Adv. Mater. Res.*, **163**, 1987-1990.
- Shao, X., Wang, H., Zhao, H. and Chang, Y. (2010), “Experimental study on multicantilever prestressed composite beams with corrugated steel webs”, *J. Struct. Eng., ASCE*, **136**(9), 1098-1110.
- Wang, F., Deng, G., Dang, X. and Yuan, W. (2015), “Seismic characteristics study of six-pylon cable-stayed bridge with corrugated steel webs”, *Energy, Environment and Green Building Materials: Proceedings of the 2015 International Conference on Energy, Environment and Green Building Materials (EEGBM 2015)*, Guilin, China, November, pp. 80-94.
- Yasukawa, Y. (2003), “Plan and design of Ritto Bridge”, *Proceedings of the 5th Japanese-German Joint Symposium on steel and Composite Bridges*, Osaka, Japan, September, pp. 143-148.
- Xu, D. and Zhao, Y. (2012), “Application of spatial grid model in structural analysis of concrete box girder bridges”, *Proceedings of the 18th Congress of International Association for Bridge and Structural Engineering (IABSE Congress Report)*, Seoul, Korea, September, Volume 18, No. 2, pp. 2009-2016.